Flexural behavior of concrete beams reinforced with BFRP bars – experimental and numerical analysis

Gean M. B. Warmling[1], Roberto D. Machado[1], Ricardo Pieralisi[1], Mauro L. Santos Filho[1]

[1]*Departamento de Construção Civil, Universidade Federal do Paraná*
Centro Politécnico – Av. Cel. Francisco H. dos Santos 100, 81530-000, Paraná, Brasil
bwgean@gmail.com, rdm@ufpr.br, ricpieralisi@ufpr.br, mauro.lacerda@ufpr.br

Abstract. This study focuses on numerical and experimental analysis of reinforced beams with Basalt Fiber Reinforce Polymer (BFRP) bars used as longitudinal and transversal reinforcements. The main characteristics of BFRP are a linear stress-strain relationship and the elasticity modulus which is lower than the conventional steel bars. Numerical analysis is conducted by carrying out nonlinear tridimensional FE models in the software DIANA TNO to study load-deflection curves of beams with BFRP as longitudinal and transversal reinforcement. In an initial analysis are established the more suitable mesh size and load step. Then, a parametric analysis considers the use of different values for compressive fracture energy and crack orientation. All the results are compared with experiments. From the obtained results, it is possible to conclude that the numerical models were capable of predict load-displacement curve for beams with BFRP reinforcement.

Keywords: BFRP, beams, numerical model, fracture energy, crack orientation.

1 Introduction

During the design of a structure, many aspects must be taken in account, for example, applied loads, material resistance, construction method, durability, etc. Conventional steel reinforcing bars used in construction are prone to corrosion due to chloride presence and concrete carbonation. These phenomena cause deterioration of the structure, consequently reducing durability. Hence, the use of fiber reinforced polymer (FRP) rebar as an alternative to steel has been gaining popularity.

FRP composites consist in combining two different materials, a reinforcing or fiber phase embedded into a matrix phase. The fibers provide strength and stiffness whereas the matrix, such as cured resin-like epoxy, holds the fibers in the intended position, providing structural integrity and shear transfer capability (Gangarao; Taly; Vijay [1]). Fibers commonly used to make FRP are glass (GFRP), aramid (ARFP) and carbon (CFRP). Recently basalt fibers have become commercially available as an alternative to glass fibers (Nanni; de Lucca; Zadeh [2]).

Mechanical behavior of FRP is different of conventional steel reinforcement, changing the design methodology. The main characteristics of BFRP are a linear stress-strain relationship and the elasticity modulus which is lower than the conventional steel bars. FRP materials have high strength in the direction of reinforcing fibers and are anisotropic, which affects shear strength, dowel effect and bond performance. Furthermore, FRP material do not yield, which means that the lack of ductility must be considered during the design procedure (ACI 440.1R-15 [3]).

Abed, El Refai and Abdalla [4] studied shear performance of BFRP reinforced beams with length of 2000mm without stirrups, considering different values for height and shear span, tested under 4 points flexure. A numerical model developed using software package ABAQUS showed good agreement with experimental results.

Fan et. al. [5] also studied beams with length of 2000mm tested under 4 points flexure. But in this case the authors used inorganic polymer concrete and BFRP as longitudinal and transversal reinforcement. A numerical model using ABAQUS using concrete damage plasticity revealed that the simulation results are in good agreement with experimental data with discrepancies of less than 5%.

Cai, Pan and Zhou [6] analyzed beams with engineered cementitious composite (ECC) and BFRP reinforcement. The authors first developed a numerical model using the software ATENA to compare with experimental results from literature. A good agreement between numerical and experimental results was observed. Then they carried out a parametric analysis to establish the effects of input parameters in the results of the numerical model.

The purpose of this study is to provide a contribution about the use of BFRP in beams through the comparison between experimental and numerical results. Three-point flexure tests were carried out in two concrete beams with longitudinal and transversal BFRP reinforcement to investigate load-deflection response. Experimental responses are compared with numerical models developed using the software DIANA 10.3. The first analysis focus on establish the more suitable mesh size and load step. Then a parametric analysis aims to study the influence of compressive fracture energy and crack orientation in the numerical response.

2 Experimental program

The experimental program consisted in two beams with BFRP as longitudinal and transversal reinforcement. Specimens are treated as Beam 1 and Beam 2. The load-deflection curves obtained in the tests are showed in the comparison with numerical models.

2.1 Test specimen

Geometry and details of reinforcement of the test specimen are shown in Fig. 1. The beams were 1100mm long with a rectangular cross section of 100mm width and 200mm height. A concrete cover of 15mm was maintained in the two tested beams. Basalt bars with diameter of 10mm were used as longitudinal reinforcement, while closed stirrups with diameter of 4mm were used as transverse reinforcement.

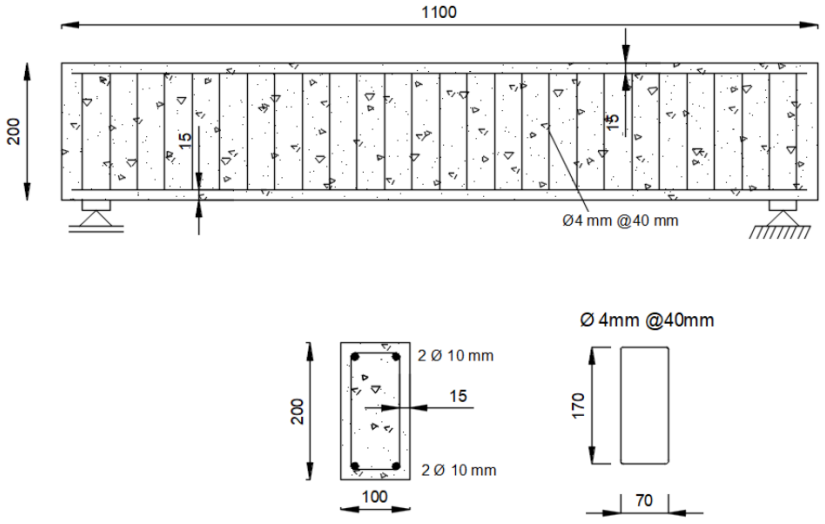

Figure 1. Geometry and reinforcing details of the tested beams

The beams were tested under three-point flexure with a span of 980 mm between supports. Midspan deflection were measured by the hydraulic press displacement and with digital image correlation (DIC). Tests were controlled by displacement.

2.2 Materials

Beams were casted using conventional concrete with average resistance of 26,25 MPa and standard deviation of 3,51 MPa. Concrete resistance was obtained through tests in standard cylinders with dimensions of 100mm x 200mm at age of 42 days. BFRP properties were provided by the manufacturer and presented tensile strength and elastic modulus of 1012,92 MPa and 52,58 GPa, respectively.

3 Finite element simulations

The flexural behavior of the BFRP reinforced beams are numerically modelled with the finite element software DIANA, version 10.3. The main objective is to observe the model behavior varying some properties. The first analysis focus on establish adequate mesh size and load step. Then, further analysis evaluates the influence of the parameters fracture energy in compression and crack orientation.

Due to symmetry, only a half of the beam is modelled with load and support plates included in the model. The vertical displacement is fixed at the support plate, on the symmetry axis perpendicular displacements are restrained. Displacement steps are applied on the load plate in the same way as in the experiments. A typical model with the boundary conditions are shown in Fig. 2.

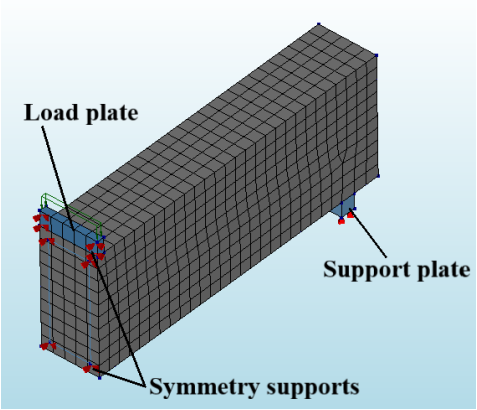

Figure 2. Typical model with the boundary conditions

Constitutive models and input parameters are presented in Tab.1. Concrete and plates were modelled mainly with a twenty-node solid brick element called CHX60, but to fit the geometry elements CPY39, CTE30 and CTP45 are also used. Reinforcements are treated as embedded.

Table 1. Constitutive models and input parameters

Parameter	Value	Reference
Concrete strength (f_c)	26,25 MPa	Experimental tests
Concrete constitutive model in compression	Parabolic	TNO DIANA BV [7]
Concrete tensile strength(f_t)	2,65 MPa	FIB Model Code 2010 [8]
Concrete constitutive model in tension	Hordijk	TNO DIANA BV [7]
Fracture tensile energy (G_t)	0,131 N/mm	FIB Model Code 2010 [8]
Compressive fracture energy (G_{fc})	32.75 N/mm	Nakamura and Higai [9]
Concrete Young's modulus (E_c)	29,66 GPa	FIB Model Code 2010 [8]
Concrete Poisson's ratio (ν_c)	0,2	NBR 6118-2014 [10]
Crack model	Total strain rotating	-

Table 2. Constitutive models and input parameters (continuation)

Parameter	Value	Reference
Reduction of Poisson's ratio	not considered	-
Reduction due lateral cracking	Vecchio e Collins (1993)	-
Lower bound reduction curve	0,7	-
Confinement model	not considered	-
BFRP constitutive model	Linear elastic	Experimental tests
BFRP Young's modulus (E_f)	52,58 GPa	Experimental tests
Steel constitutive model (plates)	Linear elastic	-
Steel Poisson ratio (plates) (ν_s)	0,3	NBR 8800-2008 [11]

3.1 Mesh discretization

This section of the research aims to study the influence of mesh discretization in the numerical solution. For this, a displacement step is set constant as 0,2 mm while meshes with 15 mm, 20 mm, 25 mm and 30 mm are tested. The accuracy of the numerical results and similarity with experimental results are observed to establish the best mesh size. Fig. 3 shows load-deflection curves for experimental results, labeled as Beam 1 and Beam 2, compared to numerical results for each mesh size.

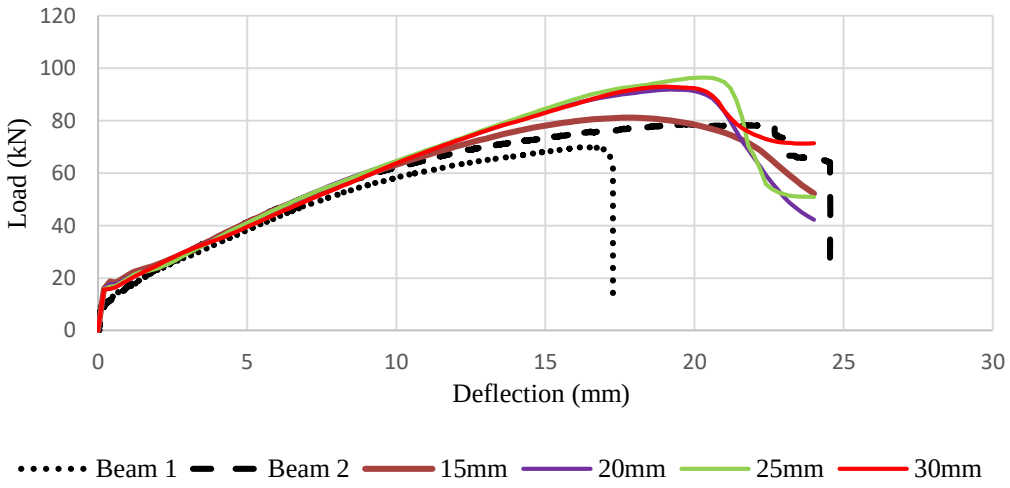

Figure 3. Load-deflection curves for different mesh sizes

It can be verified in Fig. 3 that for meshes with 20mm, 25mm e 30mm there is no significant difference between the curves. On the other hand, mesh with size of 15 mm presented a curve that differs from the others. Considering the different behavior for 15mm mesh, it was chosen to carry out parametric analysis a mesh with 20mm, that is the nearest superior size which presented solution stability compared to other mesh sizes.

3.2 Displacement step

To study the influence of displacement step in the numerical response, four different sizes were tested: 0,4mm, 0,3mm, 0,2mm and 0,1mm. For the displacement step analysis, mesh size is set with 20mm. Fig. 4 shows the response of the numerical model with different displacement steps compared with experiments.

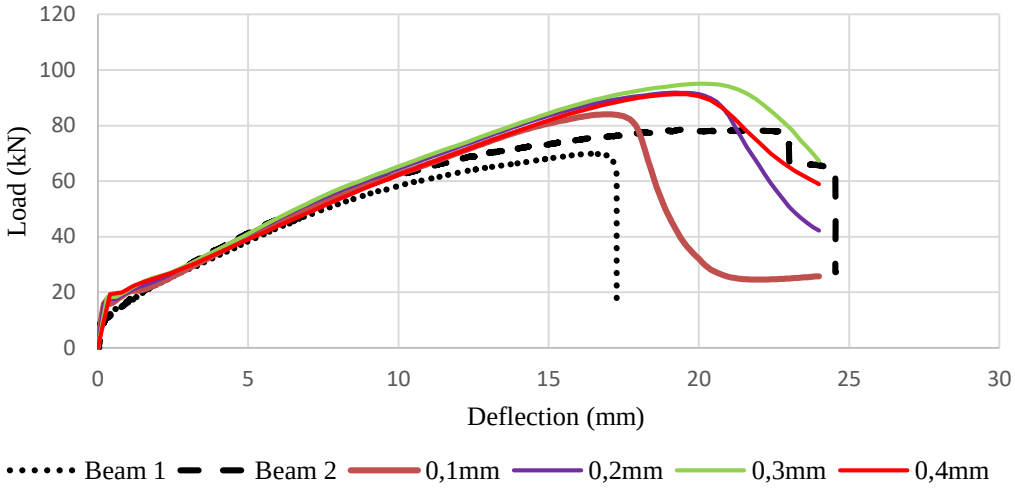

Figure 4. Load-deflection curves for different displacement steps

It can be observed in Fig. 5 that displacement step of 0,3mm present the highest values for load and displacement. Conversely, step of 0,1mm showed the lowest values for load and displacement, with a discrepancy compared to the other steps. In contrast, displacement steps of 0,2mm and 0,4mm showed very similar values for the maximum load and displacement, presenting some differences only in the post-peak portion. For carry out further analysis it is choose the intermediate displacement step of 0,2mm that has a post-peak steeper than that with 0,4mm, more similar to the experiments.

3.3 Fracture energy in compression

Compressive fracture energy (G_{fc}) can be estimated by empirical models proposed by Nakaruma and Higai [9], shown in Equations (1) and (2), and Lertsrisakulrat et. al. [12] as shown in Equation (3).

$$G_{fc} = 8{,}8\sqrt{f_c} = 45{,}08\ N/mm \tag{1}$$

$$G_{fc} = 250 G_t = 32{,}75\ N/mm \tag{2}$$

$$G_{fc} = 8{,}6 {f_c}^{1/4} = 19{,}46\ N/mm \tag{3}$$

Where f_c and G_t are, respectively, concrete compressive strength and fracture tensile energy, taken with standard values showed in Tab. 1. In Fig. 5, load-deflection curves for each value presented in the above equations (labeled as Eq.) are compared to experimental response.

It can be observed in Fig. 5 that lower values of compressive fracture energy lead to reduction in load and displacement at the peak. With values proposed by Nakamura and Higai [9], peak load is higher than the experiments and the maximum displacement value is located between that of the two tested beams. On the other hand, using the smaller value of compressive fracture energy, with the equation proposed by Lertsrisakulrat et. al. [12], peak load is almost the same of the Beam 2 and displacement is similar to Beam 1. Then, it is possible to say, for the concrete used in the experiments, that the equation proposed by Lertsrisakulrat et. al. [12] predicted better results for energy fracture in compression.

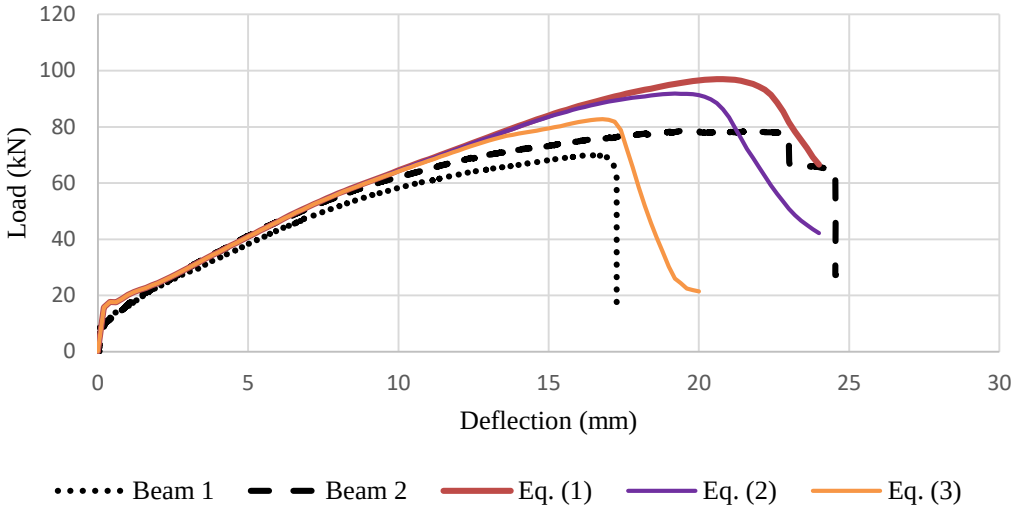

Figure 5. Load-deflection curves for different values of crack energy in compression

3.4 Crack orientation

In the numerical analysis carried out in this research, concrete was treated as total strain crack model, with cracks as smeared. Inside the smeared crack concept there two categories of cracks, fixed or rotating, related to the orientation of the crack during the entire computational process (Rots and Blaauwendraad [13]). For fixed cracks it is necessary to introduce a value for the shear retention factor (β), that is a stiffness reduction parameter. Fig. 6 shows load-displacement curves considering cracks as rotating and fixed with different values of β. In this analysis all the input parameters are set as shown in Tab. 1, except the crack model.

In Fig. 6, it can be noted that the curve for the crack treated as fixed with β=0,01 is similar with the rotating crack up to the peak load. For higher values of shear retention, it was observed an increase in load capacity. It is worth to mention that for cracks treated as fixed, it was not observed a drop in the load, which differs from experiments. For cracks treated as rotating there are a peak with a drop in the load and the load-deflection curve is more similar with the experiments. Then, it is possible to say that considering the characteristics of the tested beams, rotating crack model showed better results than fixed crack model.

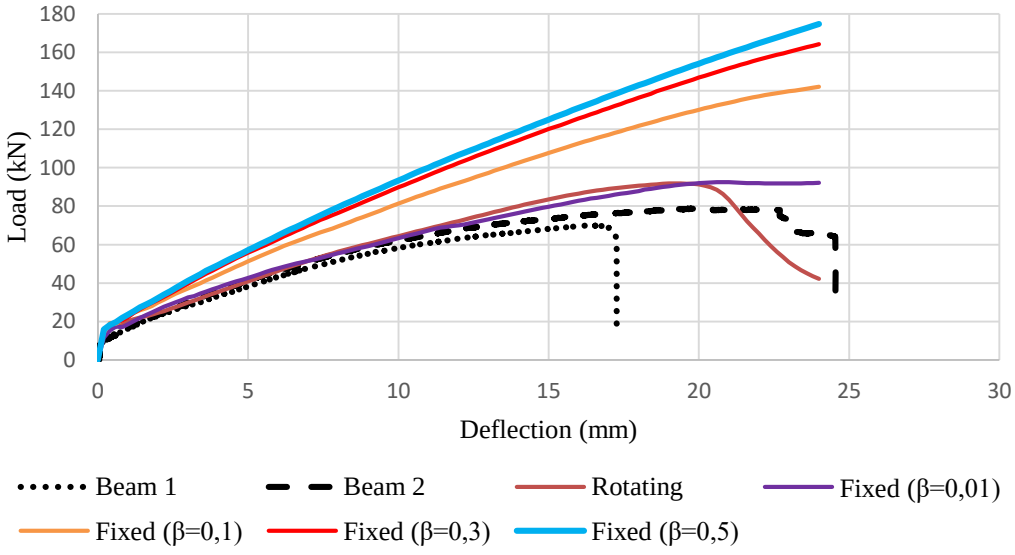

Figure 6. Load-deflection curves considering cracks as rotating and fixed

4 Conclusions

This research compared numerical and experimental results for beams reinforced with longitudinal and transversal BFRP bars. Numerical model was carried out in the software DIANA 10.3. For the mesh discretization test were chosen four different meshes, with sizes of 15mm, 20mm, 25mm and 30mm. Mesh with 15mm showed a different behavior in comparison with the other sizes, then that with 20mm was selected as the more suitable.

It was noted that the size of displacement step has an important influence in the load-deflection curve, mainly in the deflection at the peak. Four displacement steps were tested, with sizes of 0,4mm, 0,3mm, 0,2mm and 0,1mm. The smallest step (0,1mm), in this case, does not showed the best results, presenting a behavior in the load-displacement curve that was different from the other size steps. Then, a displacement step of 0,2mm was deemed more appropriate for the parametric analysis, once showed better agreement with other size steps.

To study the influence of fracture energy in compression were chosen three different equations proposed by Nakamura and Higai [9] and Lertsrisakulrat et. al.[12]. It was observed that the reduction of the fracture energy in compression lead to smaller load and displacement at the peak. Numerical model considering the smallest value for compressive fracture energy (equation proposed by Lertsrisakulrat et. al[12]), fitted better with the tested beams.

Concrete was modelling using total strain crack models, with cracks treated as smeared. Numerical models considering crack orientation as fixed or rotating were carried out. For fixed cracks different values for shear retention were tested. Rotating cracks presented a clear peak-load fitting with experiments. Fixed crack with the lowest tested value for shear retention (β=0,01) presented a load-displacement curve similar to the rotating model, except at the peak region. With the increase of shear retention factor, higher load capacity was observed. In addition, a drop in the load, representing a peak, was not observed considering cracks as fixed.

It is possible to conclude that numerical models developed in DIANA 10.3 were capable to predict load-displacement curve for beams with BFRP reinforcement. For the tested beams, the best fitting was attained using compressive fracture energy according to Lertsrisakulrat et. al.[12] and crack orientation as rotating.

Authorship statement. The authors hereby confirm that they are the sole liable persons responsible for the authorship of this work, and that all material that has been herein included as part of the present paper is either the property (and authorship) of the authors, or has the permission of the owners to be included here.

References

[1] Gangarao, H.V.S.; Taly, N.; Vijay, P.V. *Reinforced Concrete Design with FRP Composites.* 1. ed. Boca Raton, Florida: CRC Press, 2007.
[2] Nanni, A.; De Luca, A.; Zadeh, H.J. *Reinforced Concrete with FRP Bars – Mechanics and Design.* 1. ed. Boca Raton, Florida : CRC Press, 2014.
[3] ACI 440.1R-15. *ACI Guide for the Design and Construction of Structural Concrete Reinforced with Fiber-Reinforced Polymer (FRP) bars.* 1. ed. Farmington Hills: American Concrete Institute, 2015.
[4] Abed, F.; El Rafai, A.; Abdalla, S. Experimental and finite element investigation of the shear performance of BFRP-RC short beams. *Structures*, Elsevier BV, v.20, p.689-701, 2019.
[5] Fan, X.; Zhou, Z.; Tu, W.; Zhang, M. Shear behaviour of inorganic polymer concrete beams reinforced with basalt FRP bars and stirrups. *Composite Structures*, Elsevier BV, v. 255, p. 112901, 2021.
[6] Cai, J.; Pan, J.; Zhou, X. Flexural behavior of basalt FRP reinforced ECC and concrete beams. *Construction and Building Materials*, Elsevier BV, v.142, p. 423-430, 2017.
[7] TNO DIANA BV. DIANA *User's Manual – Release 10.3*. Delft: TNO DIANA BV, 2019.
[8] FIB MODEL CODE 2010. *Fib Model Code for Concrete Structures 2010*. 1. ed. Berlin, Germany: Ernst & Sohn, 2013.
[9] Nakamura, H.; Higai, T. Compressive fracture energy and fracture zone length of concrete. *Proceedings of the U.S. – Japan Seminar on Post-Peak Behavior of Reinforced Concrete Structures Subjected to Seismic Loads: Recent Advances and Challenges on Analysis and Design,* American Society of Civil Engineers, v. 1, p. 471-487, 2001.
[10] ABNT NBR 6118:2014. *Projeto de estruturas de concreto – Procedimento.* 1. ed. Rio de Janeiro: Associação Brasileira de Normas Técnicas, 2014.
[11] ABNT NBR 8800:2008. *Projeto de estruturas de aço e de estruturas mistas de aço e concreto de edifícios*. 1. ed. Rio de Janeiro: Associação Brasileira de Normas Técnicas, 2008.
[12] Lertsrisakulrat, T.; Watanabe, K.; Matsuo, M.; Niwa, J.; Experimental study on parameters in localization of concrete subjected to compression. *Journal of Materials, Concrete Structures, Pavements.* JSCE, v. 50, p. 309-321, 2001.
[13] Rots, J.G.; Blaauwendraad, J. Crack models for concrete: discrete or smeared? Fixed, multi-directional or rotating? *Heron.* TNO Institute, n.1, p-1-59, 1989.